JCBI
Journal of Computing & Biomedical Informatics
ISSN: 2710 - 1606
Volume 09 Issue 01
2025

Research Article
https://doi.org/10.56979/901/2025

Enhanced Brain Tumor Grade Classification with ConvNext: Performance Analysis

Yousuf Iqbal Bhatti[1*], Naeem Aslam[1], Ahmed Naeem[1], and Faheem Mazhar[1]

[1]Department of Computer Science, NFC-IET, Multan, Pakistan.
[*]Corresponding Author: Yousuf Iqbal Bhatti. Email: yousufiqbal7474@gmail.com

Received: April 03, 2025 **Accepted:** May 29, 2025

Abstract: The grade of a brain tumor is a crucial component of its diagnosis and aids in treatment planning. Biopsies and manual review of medical images are examples of traditional diagnostic techniques that are either invasive or may produce incorrect results. Using a contemporary convolutional neural network (CNN) architecture named ConvNext that receives magnetic resonance imaging (MRI) data, this study suggests a metho d for classifying brain tumor grades. In order to diagnose brain cancers consistently, accurately, and non-invasively, deep learning based metho ds are taking the place of invasive treatments. Data scarcity is a well-known issue with applying deep learning architectures to medical imaging. In order to attain the required accuracy and prevent overfitting, modern architectures need enormous datasets and contain enormous trainable parameters. As a result, researchers that use medical imaging data frequently use transfer learning. CNNs have recently lost ground to transformer-based designs for picture data. However, by implementing specific modifications influenced by vision transformers, freshly proposed CNNs have attained greater accuracy. A method for extracting features from the ConvNext architecture and feeding them into a fully connected neural network for final classification was presented in this article. Using pre-trained ConvNext, the proposed study obtained state-of-the-art performance on the BraTS 2019 dataset. When three MRI sequences were fed into the pre-trained CNN as three channels, the highest accuracy of 99.5% was attained.

Keywords: ConvNext; CNN; Transfer Learning; Brain Tumor Cancer; MRI

1. Introduction

A cluster of tissue that develops uncontrollably and has the potential to become fatal is called a tumor. When they emerge inside the brain, restricted by a small area inside the skull, they become considerably more harmful [1]. According to the statistics, patients from practically every demographic category have brain tumors [2]. As result, scientists from many fields work to create techniques for identifying and treating cancer. Brain tumors must be diagnosed early, just as many other illnesses [3]. The type of brain tumor, which is defined by the kind of brain cells that gave rise to it, has a significant impact on how it is treated [4]. For instance, a particular kind of brain tumor known as a meningioma develops from cells known as meninges. Likewise, a pituitary tumor is a tumorous mass that arises from the pituitary gland [5]. The most common kind of brain tumor is called glioma, and it develops inside the glial cells. This study suggests a technique for glioma diagnosis [6]. The tumor's grade is a crucial factor in the diagnosis of brain tumors. It displays the tumor's aggressiveness or the speed at which it spreads [7]. There is a high correlation between this spread rate and the anticipated number of days a patient will live. 3 [8]. Thus, in order to arrange the patient's therapy, the grade of a brain tumor is essential [9].

Tumors are categorized by the World Health Organization into four categories, ranging from Grade 1 to Grade 4. Although grade 4 cancers spread to neighboring tissues the fastest, grade 1 tumors are the least aggressive [10]. In this con-text, low-grade glioma (LGG) and high-grade glioma (HGG) are further

subdivided. Grades 3 and 4 are referred to as HGG, whereas the first two grades are classified as LGG [11]. The study suggests a method for dividing patients with glioma into LGG and HGG groups. The requirement for additional labeled data is a well-known issue when training machine/deep learning models in medical imaging [12]. Medical imaging data can be used to fine-tune models that have already been trained on generic datasets such as ImageNet. Although self-supervised pretraining using unlabeled medical data has shown better results in a number of recent studies, these techniques are computationally costly [13].

Global carbon emissions are greatly increased by computationally intensive deep learning methods, and this problem will probably get worse if researchers do not put computation efficiency first [14]. Convolutional neural network (CNN) architecture-based methods have dominated computer vision challenges for many years, producing state-of-the-art results. Numerous architectural changes have been put forth, ranging from depth-wise convolutional layers in various versions of Inception and Xception to skip connections in ResNets [15]. CNNs can now function better with ideal model sizes thanks to neura1 architecture search approaches. Transformer-based architectures, which were initially created for language problems, have recently become widely accepted for vision tasks and have demonstrated higher performance [16]. Better results have been obtained with architectures that can scale to higher image resolutions, such as the Swin transformers. Researchers have also applied them to medical imaging activities due to their exceptional performance in certain computer vision tasks [17]. However, compared to CNNs, transformer-based systems require much more computing power.

The Swin transformer has less inductive bias than CNNs, yet having a higher inductive bias than the vanilla vision transformer (ViT). Because of this, the ViT-based architecture is more computationally costly and data-hungry [18]. ConvNext,15, which has outperformed the Swin transformer on ImageNet while being computationally cheap, is used in this study to address this high computational and data requirements problem [19]. Using the pre-trained ConvNext, this study suggests a deep learning-based method that performs well with little labeled data and the limited processing capability of Google Colab's free tier. Without fie-tuning the target data for brain tumor grade classification, the features were taken from ConvNext. The outcomes demonstrate the effectiveness of the suggested strategy.

Pre-trained architectures have been used for medical imaging applications in a sizable number of studies. The pre-trained ConvNext architecture has not yet been used for this purpose in any studies that we are aware of. This study fills this gap by
classifying brain tumor grade using the most recent CNN architecture. ConvNext's transfer performance for the target task including medical images is evaluated in this study. More precisely, this study's contribution is as follows: According to this study, ConvNext's state-of-the-art performance on the goal task of classifying brain tumor grade was attained by the representations learned by its contemporary CNN architecture.

2. Related Work

Medical picture classification has historically been done using traditional machine learning techniques. However, because current designs are data-hungry, classical methods are still being proposed for medical imaging classification applications. The research that employed traditional machine algorithms for medical imaging applications are listed below. In order to determine the brain tumor grade, [20] suggested a pipeline that uses a 3D architecture built on convolutional layers to fist segment the brain's tumorous region. This area was used to extract several texture and shape-based properties.

The most discriminating features were chosen using a support vector machine (SVM) and recursive feature removal. Lastly, an accuracy of 91.27% was obtained using the extreme gradient boosting (XGBoost) classification system. Even though the study only used features from the pertinent region, the handcrafted features were unable to achieve high accuracy because they did not adequately capture the subtleties in the data. [21] graded gliomas using hand-crafted features and an XGBoost classifier following feature selection. Preprocessing, which included the Laplacian of Gaussian and wavelet transform, was the initial stage. Manually segmenting the tumorous area was the next stage. Only the tumorous area was used for feature extraction, not the entire image.

Following feature selection, the grade was finally classified with an accuracy of 83%. The Shapley value was employed in the study to evaluate how each feature contributed to the final categorization. Nevertheless, the study used manual segmentation, which is a costly and time-consuming procedure [22]. The work [23] extracted intensity, shape, and texture-based characteristics from magnetic resonance imaging (MRI) pictures using handcrafted feature extraction. Only the discriminant characteristics were retained after redundant features were removed using the correlation between various features. Lastly, the final categorization into LGG versus HGG was done using the random forest classifier. Using BraTS 2015, the study's accuracy was 91.3%. The suggested method's drawback is that it was tested on BraTS 2015, before more recent and comparable BraTS versions were accessible.

[24] suggested a method for differentiating between Grade II and Grade II gliomas. The dataset included two sequences, flid-attenuated inversion recovery (FLAIR) and contrast-enhanced T1-weighted (T1C), and 36 patients. Only the tumorous areas of the MRI scans were used to extract various textural properties. By determining the correlation between the features, the duplicate features were eliminated, leaving just the discriminating features. Grades of brain tumors were categorized using a random forest classifier [25]. A maximum accuracy of 78.1% was attained. Despite using a small dataset, the study compared the outcomes of the suggested metho with the expert radiologist's diagnosis.

Traditional machine learning techniques have the drawback of using handcrafted characteristics, which necessitate human skill to extract appropriate features. Deep learning approaches are increasingly widely used by academics because to the growing amounts of medical imaging datasets and the development of unsupervised methods that make use of generative models and unlabeled data [26]. Many projects used pre-trained CNNs for medical image categorization as deep learning-based techniques gained popularity in the second part of the previous decade. In order to overcome the small size of the target datasets and get better results than approaches that train the models from scratch, the majority of techniques make use of pre-trained models. Deep learning-based methods have been used to problems using medical imaging in the following papers. [27] carried out preprocessing, which included filing the bias field, to lessen the impact of problems that arose during the MRI scan capture process. The image is then smoothed by applying the Gaussian filter. A stack of four slices, representing the four MRI sequences, is used for preprocessing before being fed into the long short-term memory (LSTM) model. The last fully connected layer divides photos into HGG and LGG categories. The study's highest accuracy on BraTS 2018 was 98%. The work presented a novel method for processing various MRI sequences utilizing a sequence model. [28] extracted deep features from MRI data using the pre-trained InceptionV3 CNN. The study used contrast enhancement in the preprocessing stage prior to feature extraction. The suggested method additionally used a local binary pattern variation to extract handcrafted features. The next pipeline step, feature selection using particle swarm optimization, received the concatenated deep and handmade features. The study's highest accuracy on BraTS 2017 was 96.9%. The handcrafted and deep features were combined in the study. However, by using depth wise separable convolutions, the Xception architecture achieved higher ImageNet accuracy.

The ImageNet pre-trained ResNet-152 was used in study to classify the grade of brain tumors. The original architecture's classifier layer was swapped out with a SoftMax classifier. For the BraTS 2019 dataset, [29] employed a deep architecture and obtained a 98.85% accuracy rate. In order for the proposed CNN to extract the pertinent imaging characteristics from the MRI data, [30] suggested a novel CNN design modulated by the Gabor filter. The study applied the leave-one-patient strategy to improve the dependability of the findings. The outcomes were contrasted with CNNs that had already been trained, such as AlexNet, VGG-19, InceptionV1, and ResNet34. All of the pre-trained CNNs were surpassed by the suggested architecture. Even if [31] offered a novel approach to the traditional CNN architecture, a comparison with the outcomes of more recent CNN designs could improve the study's dependability.

To diagnose brain cancers into three categories: normal versus abnormal, classification of glioma, pituitary, and meningioma types, and classification of grades I-IV, [32] suggested three innovative CNN architectures. The datasets utilized were REMBRANDT for grade classification, Figshare CE-MRI for type classification, and Kaggle brain tumor type classification for normal versus abnormal. [33] used a median filter for image quality improvement and noise reduction as preprocessing. To expand the dataset size, traditional data augmentation methods such as image scaling and angle rotation were applied. The amount of the dataset and the difficulty of the task determined the architecture's complexity. The grid

search was used to find the ideal hyperparameters. Although the transformer architecture's variation vision transformer yielded outstanding results for the picture classification challenges, it was first suggested for natural language data. In order to extract features for the study's target job of classifying brain tumor grades, a pre-trained CNN with a contemporary architecture (ConvNext Base) is used. The design decisions and training techniques that enabled the ConvNext architecture to reach cutting-edge performance are shown in Figure 1.

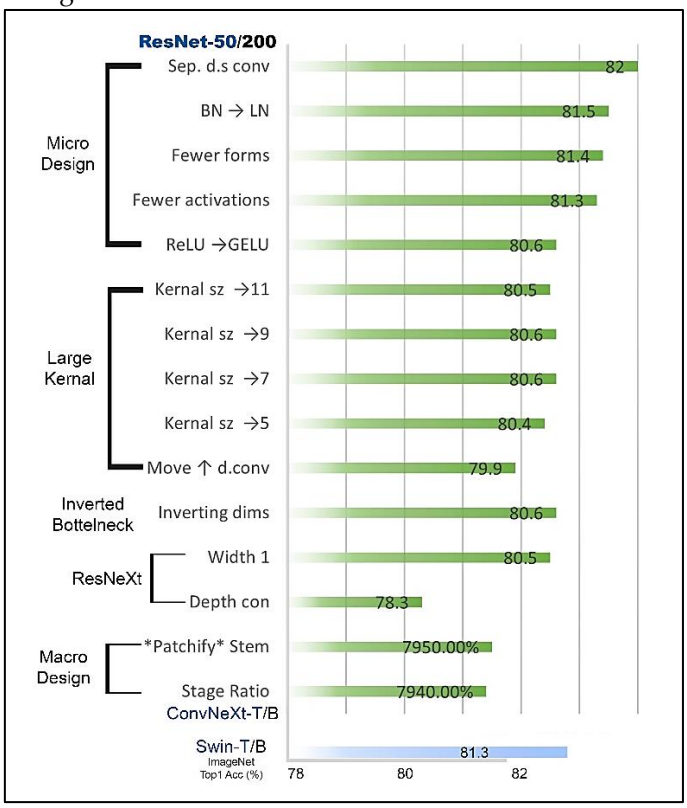

Figure 1. Transformer-based architectures serve as an inspiration for ConvNext's architecture and training technique.

3. Research Methodology

The present longitudinal study employs the suggested CNN base d metho d to classify brain tumor grade utilizing an existing, publicly accessible dataset. In the spring of 2024, it was carried out at the COMSATS University Islamabad, Lahore Campus, Pakistan, in the Machine Perception & Visual Intelligence Research Group. BraTS 2019, the study's publicly accessible dataset, was made available in 2019. Figure 2 displays the block diagram for the suggested approach. The pipeline's initial stage involved flagging the tumorous slices. Following that, just the tumorous slices' characteristics were removed, giving the classifier slices with either an LGG or HGG tumor. The study employed ConvNext Base, the standard version of ConvNext, to extract feature s by freezing each layer. A global average pooling layer that extracted one feature p er feature map to ok the role of the top model from the pre-trained ConvNext, yielding 1024 features in total. Ultimately, a fully connected neural network was given the features to classify the data into LGG and HGG The study's dataset and technique are thoroughly explained in the subsections Dataset," Deep feature extraction" and" Classification".

3.1. Dataset

The study use the BraTS 2019 dataset for brain tumor grading utilizing the features taken from ConvNext. BraTS is a well-known publicly accessible dataset, and its several iterations provide a standard against which to compare methods [34]. A mapping of the BraTS 2017, 2018, 2019, and 2020 datasets was supplied as part of the BraTS 2020 dataset. 210 of the 259 HGG patients are shared throughout the three datasets, and 49 more patients are included in the BraTS 2019 dataset [35]. There is only one extra patient for LGG patients in BraTS 2019, and 75 cases are identical across the three datasets [36].

While the BraTS 2014–2016 cases are eliminated since they are not annotated by qualified radiologists, the BraTS 2012 and 2013 cases are already included in these editions (2017 or later) [37]. The

dataset is even more imbalanced because BraTS 2020 has 34 more HGG instances than BraTS 2019. This analysis led to the use of BraTS 2019 in this study [38]. Each of the dataset's 76 LGG and 259 HGG instances has four sequences (T1, T2, T1 T1C, and FLAIR) and one ground-truth value, which is the result of experienced radiologists' hand tumor segmentation. Every MRI scan for a sequence has 155 slices, each measuring 240 by 240 pixels [39].

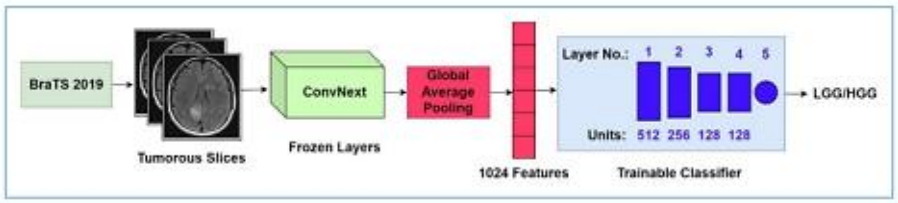

Figure 2. Diagram with blocks illustrating the suggested approach

The acquisition methodology is 2D sagittal or axial for T1, with slices that are 1–6 mm thick; 3D and typically 1 mm thick for T1C; 2D in axial orientation for T2, with slices that are 2–6 mm thick; and 2D in all orientations for FLAIR, with slices that are 2–6 mm thick [40]. Different sections of the tumor (edema, necrotic region, enhancing, and non-enhancing core) were identified using various sequences or combinations during manual segmentation (conducted by the dataset suppliers). The delineations made by different radiologists for each case were combined to create a single, cohesive segmentation [41].

The suggested approach did not carry out additional preparation on the dataset, which was previously preprocessed. The dataset providers used image registration and skull stripping as preprocessing techniques. Since the T1C sequence has the maximum spatial resolution, it was used as the reference for registration using rigid transformation. The skull signal was then eliminated by skull stripping.

3.2. Features Extraction and Classification

The weights of the ConvNext (Base version) convolution base, which were pre-trained on the ImageNet dataset, were used to extract features in the suggested technique. As a result, just the ConvNext architecture's convolution foundation was utilized; the top model, which included logistic regression and optional fully linked layers, was dropped. Each magnetic resonance slice produced 1024 features thanks to the application of global average pooling. Only the slices containing the tumorous pixels were used, rather than all of the slices.

The dataset's ground truth segmentation was used to retrieve these tumorous slices. Without carrying out any additional preprocessing steps, the tumorous slices were put into the ConvNext that had already been trained. Each slice was repeated three times to fill the input layer's three channels and match the input dimensions of the pretrained ConvNext.

Table 1. Classifier network structure.

Layer Type	NO of units	Activations
Dense	128	ReLu
Dense	256	ReLu
Dense	512	ReLu
Dense	1	Sigmoid

Global average pooling and the frozen layers in the ConvNext convolution base were used to extract the features, which were then input into a fully connected neural network with 754,945 trainable parameters. The layers of the classifier network, the units within each layer, and the activation functions employed are displayed in Table 1.

Two different kinds of experiments were conducted. In the first, the model was trained for 500 epochs without the validation set in order to evaluate the convergence behavior. The trajectory of the model to convergence for each setting was shown with the aid of checkpoints that were saved after each epoch and for which the test set accuracy was assessed following training. Tables 4 and 7 offer helpful insight into the optimal checkpoints for various input settings.

Table 2. Configurations for the Classification's Hyper-Parameters

Parameter	Value

Epoch's	500
BatchSize	64
Learningrate	0.001
Optimizer	Adam
Checkpoint	Following each Epoch

This research builds on a previous [42] that was carried out to determine the best pre-training approach. The study included two models: a simple model and a sophisticated one. Other hyperparameters, like the precise number of layers and units per layer, were adjusted empirically. This study used the complex model (Table 1) and kept the same hyperparameters. The classification's hyperparameter setup is displayed in Table 2.

3.3. Statistical Analysis

The percentage of correctly categorized instances in the test set is known as the accuracy. To appropriately portray the results in the presence of imbalanced classes, this study computes the class-specific accuracies using the measures of sensitivity (TPR) and specificity (TNR) in addition to the overall accuracy. Furthermore, the suggested method's performance was evaluated using the AUC metric, which provides a thorough overview of the model's capacity for class distinction, independent of decision boundaries. These metrics were computed using Python's scikit-learn package. A horizontal bar graph was used to compare the outcomes for each sequence combination. To better visualize the performance difference between the separate and combined sequences, bars were created for each measure, and the bars for the metrics of each sequence combination were grouped. The results were shown using Python's Matplotlib tool.

3.4. Experimental Results

Only the slices identified as tumorous by radiologists were employed, and 2D slices rather than 3D volumes were used to enhance the number of samples for training. Consequently, slices of 17,224 HGG and 4926 LGG were produced. This data was split into training and test sets using an 80–20 class balanced split in order to observe the training progress and convergence behavior. This left 17,720 samples for training and 4430 for testing, with each slice (sample) having a size of 240 × 240. Ten percent of the training set was devoted to the validation set for the second series of experiments. This indicates that while 15,948 slices were utilized to train the model, 1772 slices were kept aside for validation. The train, test, and validation sets' images and slice are displayed in Table 3.

Table 3. Images or slicing from the test, validation, and train sets

Clases	Training set	Validation set	Test set	Total Images
High grade glioma	12401	3445	1378	17224
Low grade glioma	3547	985	394	4926

Every feasible combination of the sequences was used in the experiments. The input was restricted to having exactly three channels since the pre-trained ConvNext was used for feature extraction. As a result, only a mix of the three sequences could be applied. One channel of the input tensor was occupied by each sequence.

4. Results

Every possible combination of any three sequences was tested in the experiments. Accuracy, sensitivity, specificity, and area under the curve (AUC) are the metrics used for evaluation. It has been decided to treat HGG as the positive class and LGG as the negative class. As a result, specificity is the proportion of correctly categorized LGG cases, and sensitivity is the proportion of correctly recognized HGG examples. In each experiment, the model was trained for 500 epochs, with checkpoints saved at the end of each epoch to examine the training progression and convergence behavior. Table 4 displays each experiment's best outcomes (accuracy, sensitivity, specificity, and AUC) for each combination of sequences.

The table's highest accuracy is indicated in bold. The training epochs were once more set to 500 in the second series of trials (grade classification using train, test, and validation sets). However, due of the early stopping with a patience of 20, the training ended significantly earlier for each experiment. Table 5 displays each experiment's test set results (accuracy, sensitivity, specificity, and AUC) for each combination of sequences. The table's highest accuracy is indicated in bold.

In both kinds of studies, the combination of T1, T1C, and FLAIR sequences produced the highest accuracy (99.61% and 99.5%). Using the FLAIR sequence, the combination of T1, T1, T1C, and FLAIR produced the lowest accuracy (99.37% and 99.03%). The combinations including T1 and T1C yielded the top two best accuracies. These findings are explained by manual segmentation of the magnetic resonance images in the BraTS dataset. While the radiologists labeled the data using all the sequences, they segmented various tumor substructures using T1 and T1C

4.1. Comparative analysis with research employing BraTS 2017 or later

Since BraTS 2017 and 2018 are the datasets that are most similar to BraTS 2019, while the earlier BraTS datasets are different, the study outcomes (of experiments using a validation set) have been compared with those utilizing these two datasets. Only a small portion of the BraTS 2013 and 2017 data—60 photos for training and 100 for testing—was included in the study34. It is therefore excluded from the comparison, even though it claimed 99% accuracy. Table 4 presents a comparison between the suggested approach and the research that used BraTS 2017 or later for brain tumor grading.

Table 4. Comparative analysis with research employing BraTS 2017 or later

Study	Model/Method	Dataset	Key Techniques	Accuracy
[27]	LSTM model with sequence of 4 slices	BraTS 2018	Bias field correction, Gaussian smoothing, sequence modeling	98.0%
[28]	InceptionV3 + Handcrafted Features + PSO	BraTS 2017	Deep + LBP features, feature selection using particle swarm optimization	96.9%
[29]	ResNet-152 with SoftMax classifier	BraTS 2019	Replaced classifier, fine-tuned on MRI slices	98.85%
[30]	Gabor-filter modulated CNN	BraTS (Not Specified)	Compared with AlexNet, VGG-19, ResNet34	>98%
[31]	EfficientNet + Multi-class Classification	BraTS (Unclear)	Multi-class tumor type classification	>98%
Proposed	ConvNext Base + Fully Connected Neural Network	BraTS 2019	Feature extraction from frozen ConvNext, combined sequences as 3 input channels	99.5%

4.2. Ablation Study

In order to provide a three-channel input, studies have utilized separate sequences and duplicated the same slice three times. The ablation study's goal was to observe the outcome of using just one sequence. The optimum sequence was determined by evaluating each of the four sequences.

Table 5. Evaluation of MRI Sequences

MRI Sequence	Accuracy (%)	Sensitivity (TPR)	Specificity (TNR)	AUC	Observation
T1	99.12	High	High	High	Highest accuracy among single sequences
T2	~98.45	Moderate	Moderate	Moderate	Slightly less effective

T1C	~98.87	High	Moderate	Moderate	Close second to T1; strong discriminative power
FLAIR	~97.91	Low	Low	Lower	Weakest individual sequence

Additionally, compared to the individual sequences, it required more epochs for all sequence combinations to converge (get the highest accuracy). Radiologists manually segment brain tumors using various MRI sequences, each of which has complementing information.

4.3. Discussion

The outcomes shown that when three distinct MRI sequences were fed into the CNN, the suggested approach outperformed the SOTA and attained higher accuracy. Numerous research examined the outcomes of grading brain tumors using individual sequences and their combinations using BraTS databases. Using the BraTS 2017 dataset, the study42 employed convolutional autoencoders for brain tumor grading. The convolutional autoencoders were fine-tuned on real images after pre-training on synthetic images produced by the generative adversarial network. The T1C, T2, and 1 FLAIR sequences were employed alone and in combination. The combination of these three sequences produced the best and average results, but T1C produced the best accuracy for individual sequences.

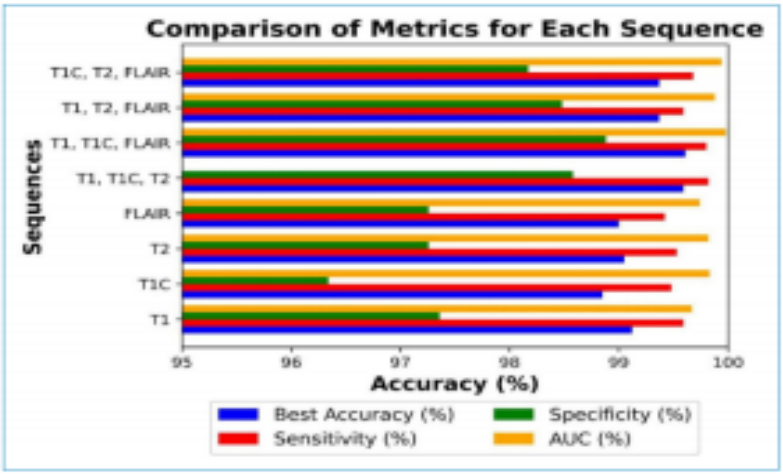

Figure 3. Illustration of the observations using 500 epoch

The outcomes shown that when three distinct MRI sequences were fed into the CNN, the suggested approach outperformed the SOTA and attained higher accuracy. Numerous research examined the outcomes of grading brain tumors using individual sequences and their combinations using BraTS databases. Using the BraTS 2017 dataset, the study42 employed convolutional autoencoders for brain tumor grading. The convolutional autoencoders were fine-tuned on real images after pre-training on synthetic images produced by the generative adversarial network. The T1C, T2, and FLAIR sequences were employed alone and in combination. The combination of these three sequences produced the best and average results, but T1C produced the best accuracy for individual sequences. The study's findings were contrasted with those of other recent research projects that employed deep learning and standard machine learning methods.

The studies classified the grade of brain tumors using traditional machine learning techniques. Shape-based, histogram-based, and texture features were employed in the study, along with a logistic regression classifier. At the same time, a random forest classifier produced the highest accuracy. In order to classify grades, the study employed textural data, which were then fed into standard neural networks following feature selection. With the exception of two research that employed convolutional autoencoders and LSTMs for grade classification,

The research suggested new CNN architectures, and for grade classification, it combined dominant rotating local binary pattern features with deep features taken from pre-trained InceptionV3. In order to give the learnt features rotation and scale invariance, the study employed a new CNN in which the convolutional layers were modulated by the Gabor filter bank. By employing generative adversarial networks (GAN) to create synthetic data and semi-supervised learning to estimate the labels of unlabeled

data, the study expanded the dataset size. After choosing the best characteristics, the study40 employed deep features and fed them to the SoftMax.

5. Conclusion and Future work

The research community was able to create and train the ConvNext architecture and attain state-of-the-art performance thanks to the Swin transformer's success. The CNN architecture is better suited for the image data because of its stronger inductive bias. ConvNext is an appropriate architecture for medical imaging workloads with reduced dataset sizes because of these features. The pre-trained ConvNext architecture is used in this work to classify the grade of brain tumors. Following the extraction of the BraTS 2019 dataset's features from the ConvNext architecture, the study employed linear probing. The effectiveness of the representations learned from the pre-trained ConvNext architecture was shown by the better results in accuracy, sensitivity, specificity, and AUC on the target task of brain tumor grade classification. ConvNext representations for a target medical image task were used in the study to present the findings. For a thorough examination encompassing numerous imaging modalities, organs, and anomalies, more research is necessary. The study must use datasets of varying sizes, ranging from small to medium to large, in order to guarantee generalizability. Additionally, it is necessary to examine the effectiveness of several iterations of the ConvNext architecture. Numerous studies have recently employed domain-adapted pre-training to outperform generic dataset pre-trained models. The domain gap between the generic dataset and the target dataset (such as MRI) could be bridged by the in-domain data pretraining that followed the generic dataset pretraining (e.g. ImageNet). Comparing ConvNext's performance following domain-adaptive pre-training versus that following generic dataset pre-training would be intriguing. Another compute-efficient training strategy that produces a model with significantly fewer parameters while maintaining equivalent accuracy is the lottery ticket method and its variations. Investigating a pretrained model's performance on a target task using these techniques is worthwhile. Finally, several research have slightly modified the pre-trained models to accommodate the target data with more channels in the data (e.g. MRI). Investigating the computationally effective techniques recommended in this part while utilizing all the sequences throughout the target categorization is required since doing so yields comprehensive knowledge about a subject.

References

1. Lamba, K., Rani, S., Khan, M.A., Shabaz, M.: Re-incep-bt-: Resource-efficient inceptor model for brain tumor diagnostic healthcare applications in computer vision. Mobile Networks and Applications, 1–15 (2024)
2. Amin, J., Sharif, M., Haldorai, A., Yasmin, M., Nayak, R.S.: Brain tumor detection and classification using machine learning: a comprehensive survey. Complex & intelligent systems 8(4), 3161–3183 (2022)
3. Miller, K.D., Ostrom, Q.T., Kruchko, C., Patil, N., Tihan, T., Cioffi, G., Fuchs, H.E., Waite, K.A., Jemal, A., Siegel, R.L., et al.: Brain and other central nervous system tumor statistics, 2021. CA: a cancer journal for clinicians 71(5), 381–406(2021)
4. Palmieri, A., Valentinis, L., Zanchin, G.: Update on headache and brain tumors. Cephalalgia 41(4), 431–437 (2021)
5. Ullah, M.S., Khan, M.A., Almujally, N.A., Alhaisoni, M., Akram, T., Shabaz, M.: Brainnet: a fusion assisted novel optimal framework of residual blocks and stacked autoencoders for multimodal brain tumor classification. Scientific Reports 14(1), 5895 (2024)
6. Ahmed Hamza, M., Abdullah Mengash, H., Alotaibi, S.S., Hassine, S.B.H., Yafoz, A., Althukair, F., Othman, M., Marzouk, R.: Optimal and efficient deep learning model for brain tumor magnetic resonance imaging classification and analysis. Applied Sciences 12(15), 7953 (2022)
7. Chanchlani, A.S., Thakare, V.M., Wadhai, V.M., Gawali, D.H., Patil, M.: An efficient system for predictive analysis on brain cancer using machine learning and deep learning techniques. In: Designing Intelligent Healthcare Systems, Products, and Services Using Disruptive Technologies and Health Informatics, pp. 229–244. CRC Press, ??? (2022)
8. Mazhar, F., Aslam, N., Naeem, A., Ahmad, H., Fuzail, M., Imran, M.: Enhanced diagnosis of skin cancer from dermoscopic images using alignment optimized convolutional neural networks and grey wolf optimization. Journal of Computing Theories and Applications 2(3) (2025)
9. Ullah, M.S., Khan, M.A., Masood, A., Mzoughi, O., Saidani, O., Alturki, N.: Brain tumor classification from mri scans: a framework of hybrid deep learning model with bayesian optimization and quantum theory-based marine predator algorithm. Frontiers in Oncology 14, 1335740 (2024)
10. Ariful Islam, M., Mridha, M., Safran, M., Alfarhood, S., Mohsin Kabir, M.: Revolutionizing brain tumor detection using explainable ai in mri images. NMR in Biomedicine 38(3), 70001 (2025)
11. Kudus, K., Wagner, M., Sheng, M., Bennett, J., Liu, A., Tabori, U., Hawkins, C., ertl-wagner, B., Khalvati, F.: Segmentation-free pretherapeutic assessment of braf-status in pediatric low-grade gliomas. medRxiv, 2025–01 (2025)
12. Disci, R., Gurcan, F., Soylu, A.: Advanced brain tumor classification in mr images using transfer learning and pre-trained deep cnn models. Cancers 17(1), 121 (2025)
13. Huang, Z., Duan, J., Xie, Y., Liu, Y.: Udnet: Unified deep network based on transformer and multi-stage fusion for brain tumor classification from undersampled mri. Neurocomputing 619, 129109 (2025)
14. Panthakkan, A., Anzar, S., Mansoor, W.: Unleashing the power of efficientnetconvnext concatenation for brain tumor classification. In: 2023 15th Biomedical Engineering International Conference (BMEiCON), pp. 1–5 (2023). IEEE
15. Cui, S., Ji, W., Zhang, L., Wang, R., Wang, A.: Cdkn2a/b gene classification method for glioma with attention convnext. In: Proceedings of the 2023 3rd International Conference on Bioinformatics and Intelligent Computing, pp. 285–288 (2023)
16. Techa, C., Ridouani, M., Hassouni, L., Anoun, H.: Automated alzheimer's disease classification from brain mri scans using convnext and ensemble of machine learning classifiers. In: International Conference on Soft Computing and Pattern Recognition, pp. 382–391 (2022). Springer
17. Yin, Z., Gao, H., Gong, J., Wang, Y.: Wd-unext: Weight loss function and dropout u-net with convnext for automatic segmentation of few shot brain gliomas. IET Image Processing 17(11), 3271–3280 (2023)
18. Wang, S., Gao, Z., Liu, D.: Swin-gan: generative adversarial network based on shifted windows transformer architecture for image generation. The Visual Computer 39(12), 6085–6095 (2023)
19. Jiang, Y., Zhang, Y., Lin, X., Dong, J., Cheng, T., Liang, J.: Swinbts: A method for 3d multimodal brain tumor segmentation using swin transformer. Brain sciences 12(6), 797 (2022)
20. Xu, C., Peng, Y., Zhu, W., Chen, Z., Li, J., Tan, W., Zhang, Z., Chen, X.: An automated approach for predicting glioma grade and survival of lgg patients using cnn and radiomics. Frontiers in Oncology 12, 969907 (2022)
21. Qin, C., Hu, W., Wang, X., Ma, X.: Application of artificial intelligence in diagnosis of craniopharyngioma. Frontiers in Neurology 12, 752119 (2022)

22. Deng, F., Liu, Z., Fang, W., Niu, L., Chu, X., Cheng, Q., Zhang, Z., Zhou, R., Yang, G.: Mri radiomics for brain metastasis sub-pathology classification from non-small cell lung cancer: a machine learning, multicenter study. Physical and Engineering Sciences in Medicine 46(3), 1309–1320 (2023)
23. Mushtaq, S., Malik, K. R., Ahmad, Z., & Sajid, M. (2023). A Deep Learning Based Approach to Enhance Object Edge Detection for Office Surveillance System. Journal of Computing & Biomedical Informatics, 6(01), 270-286.
24. Zhao, S.-S., Feng, X.-L., Hu, Y.-C., Han, Y., Tian, Q., Sun, Y.-Z., Zhang, J., Ge, X.-W., Cheng, S.-C., Li, X.-L., et al.: Better efficacy in differentiating who grade ii from iii oligodendrogliomas with machine-learning than radiologist's reading from conventional t1 contrast-enhanced and fluid attenuated inversion recovery 1images. BMC neurology 20, **1**–10 (2020)
25. Ahmad, H., Sajid, M., Mazhar, F., & Fuzail, M. (2025). Mapping Unseen Connections: Graph Clustering to Expose User Interaction Patterns. Journal of Future Artificial Intelligence and Technologies, 1(4), 474-496.RD
26. Mateen, A., Malik, K. R., Ahmad, Z., & Sajid, M. (2023). Revolutionizing news discovery: YOLOv7 empowers real-time headline extraction from video content. Journal of Computing & Biomedical Informatics, 6(01), 300-317.
27. Athisayamani, S., Antonyswamy, R.S., Sarveshwaran, V., Almeshari, M., Alzamil, Y., Ravi, V.: Feature extraction using a residual deep convolutional neural network (resnet-152) and optimized feature dimension reduction for mri brain tumor classification. Diagnostics 13(4), 668 (2023)
28. Sajid, M., Malik, K. R., Khan, A. H., Iqbal, S., Alaulamie, A. A., & Ilyas, Q. M. (2025). Next-generation diabetes diagnosis and personalized diet-activity management: A hybrid ensemble paradigm. PloS one, 20(1), e0307718.
29. Hafeez, H.A., Elmagzoub, M.A., Abdullah, N.A.B., Al Reshan, M.S., Gilanie, G., Alyami, S., Hassan, M.U., Shaikh, A.: A cnn-model to classify low-grade and high-grade glioma from mri images. IEEE Access 11, 46283–46296 (2023)
30. Hafeez, Y., Memon, K., Al-Quraishi, M.S., Yahya, N., Elferik, S., Ali, S.S.A.: Explainable ai in diagnostic radiology for neurological disorders: A systematic review, and what doctors think about it. Diagnostics 15(2), 168 (2025)
31. Zulfiqar, F., Bajwa, U.I., Mehmood, Y.: Multi-class classification of brain tumor types from mr images using efficientnets. Biomedical Signal Processing and Control 84, 104777 (2023)
32. Gull, S., Akbar, S., Naqi, S.M.: A deep learning approach for multi-stage classification of brain tumor through magnetic resonance images. International Journal of Imaging Systems and Technology 33(5), 1745–1766 (2023)
33. Ayana, G., Dese, K., Abagaro, A.M., Jeong, K.C., Yoon, S.-D., Choe, S.-w.: Multistage transfer learning for medical images. Artificial Intelligence Review 57(9), 232 (2024)
34. Sabir, A. A., Saleem, U., Aslam, N., Rehman, A., Sajid, M., & Fuzail, M. (2023). Enhancing Human Activity Analysis in Video Surveillance with Recurrent Neural Networks. Journal of Computing & Biomedical Informatics, 5(01), 1-12.
35. Sajid, M., Aslam, N., Abid, M. K., & Fuzail, M. (2022). RDED: recommendation of diet and exercise for diabetes patients using restricted boltzmann machine. VFAST Transactions on Software Engineering, 10(4), 37-55.
36. Mazhar, F., Aslam, N., Sajid, M., Naeem, A., & Fuzail, M. (2025). Leveraging Improved YOLOv10 for High-Performance License Plate Recognition in Challenging Mass Transit Environments. Journal of Computing & Biomedical Informatics, 9(01).
37. Ullah, S., Iqbal, N., Khan, A. H., Sajid, M., Ahmad, Z., Ahmad, H., & Hussain, M. (2023). Empowering agriculture: a green revolution with internet of energy-driven farm energy management for sustainable and eco-friendly practices. Journal of Population Therapeutics and Clinical Pharmacology, 30(19), 975-992.
38. Hernandez-Gutierrez, F.D., Avina-Bravo, E.G., Zambrano-Gutierrez, D.F., Almanza-Conejo, O., Ibarra-Manzano, M.A., Ruiz-Pinales, J., Ovalle-Magallanes, E., Avina-Cervantes, J.G.: Brain tumor segmentation from optimal mri slices using a lightweight u-net. Technologies 12(10), 183 (2024
39. Kuroda, H., Okita, Y., Arisawa, A., Utsugi, R., Murakami, K., Hirayama, R., Kijima, N., Arita, H., Kinoshita, M., Fujimoto, Y., et al.: Cerebral blood flow and histological analysis for the accurate differentiation of infiltrating tumor and vasogenic edema in glioblastoma. PloS one 20(1), 0316168 (2025
40. Ghafouri, A., Biros, G.: Single-scan mpmri calibration of multi-species brain tumor dynamics with mass effect. In: International Workshop on Simulation and Synthesis in Medical Imaging, pp. 187–196 (2024). Springer
41. Cerina, V., Rui, C.B., Di Cristofori, A., Ferlito, D., Carrabba, G., Giussani, C., Basso, G., De Bernardi, E.: Implication of tumor morphology and mri characteristics on the accuracy of automated versus human segmentation of gbm areas. Scientific Reports 15(1), 2160 (2025)
42. Mehmood, Y., Bajwa, U.I., Sun, X.: Resource-efficient domain adaptive pretraining for medical images. arXiv preprint arXiv:2204.13280 (2022).